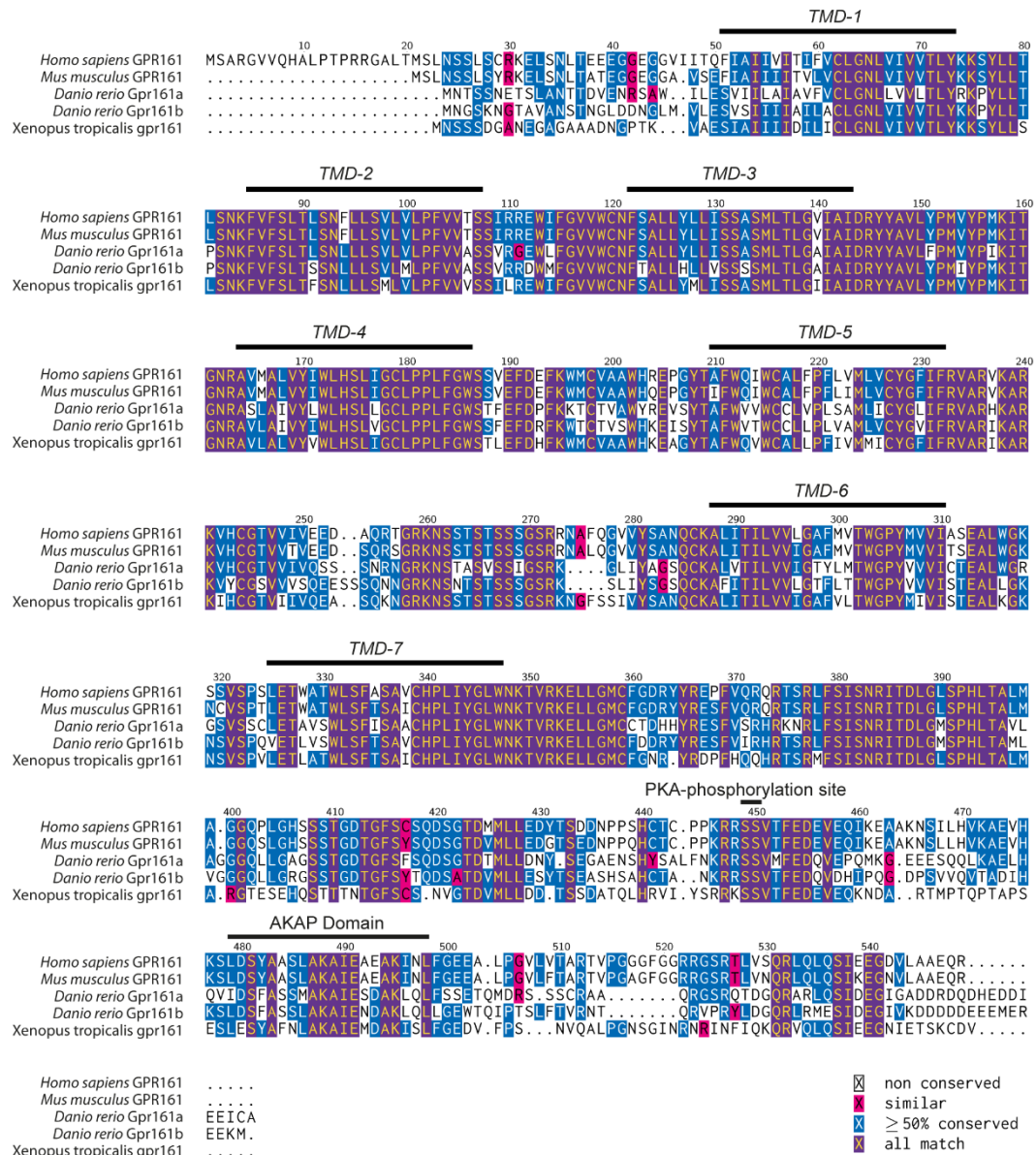
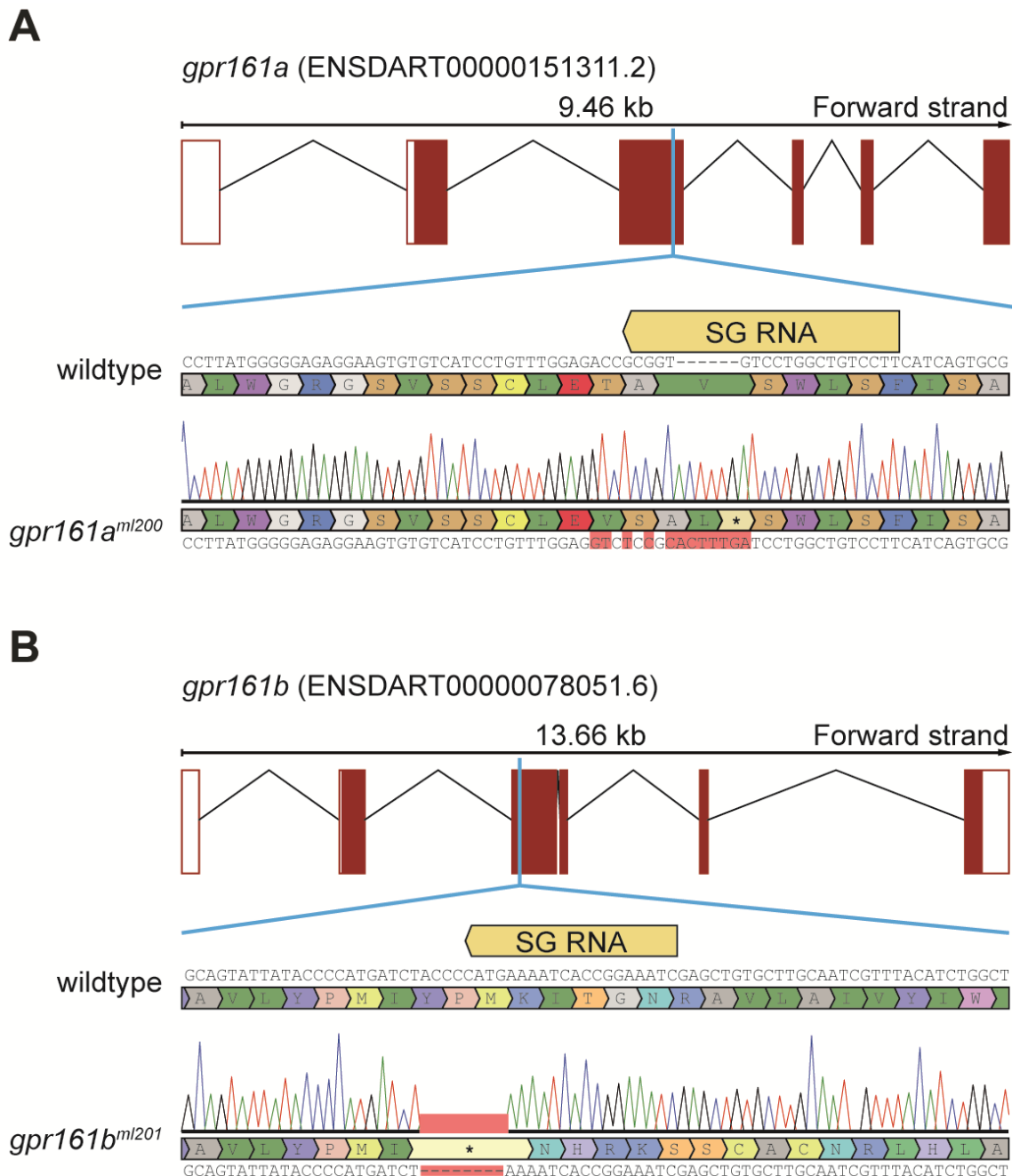


## SUPPLEMENTARY INFORMATION

## Supplementary Figures

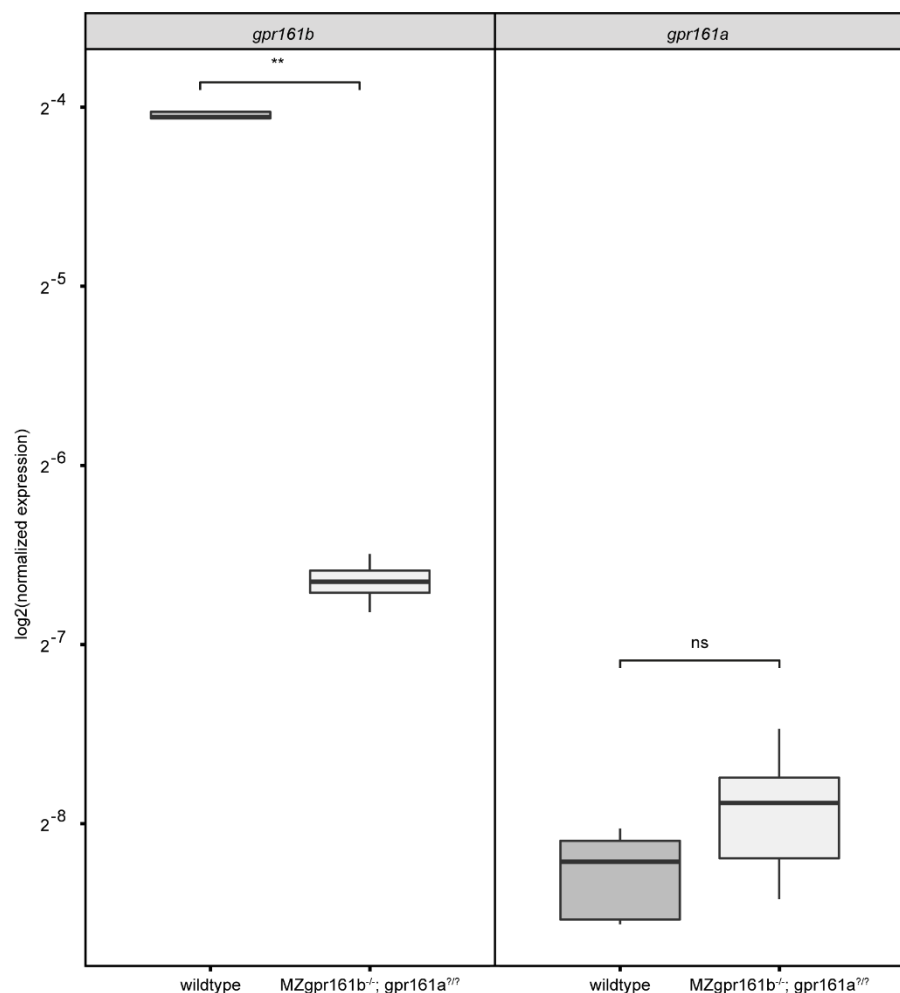
**Figure S1. Multiple Sequence Alignment.**

The sequences of the *Homo sapiens*, *Mus musculus*, *Danio rerio* and *Xenopus tropicalis* Gpr161 proteins were aligned using MUSCLE (Edgar, 2004). Transmembrane domains (TMDs) and conserved residues are indicated.



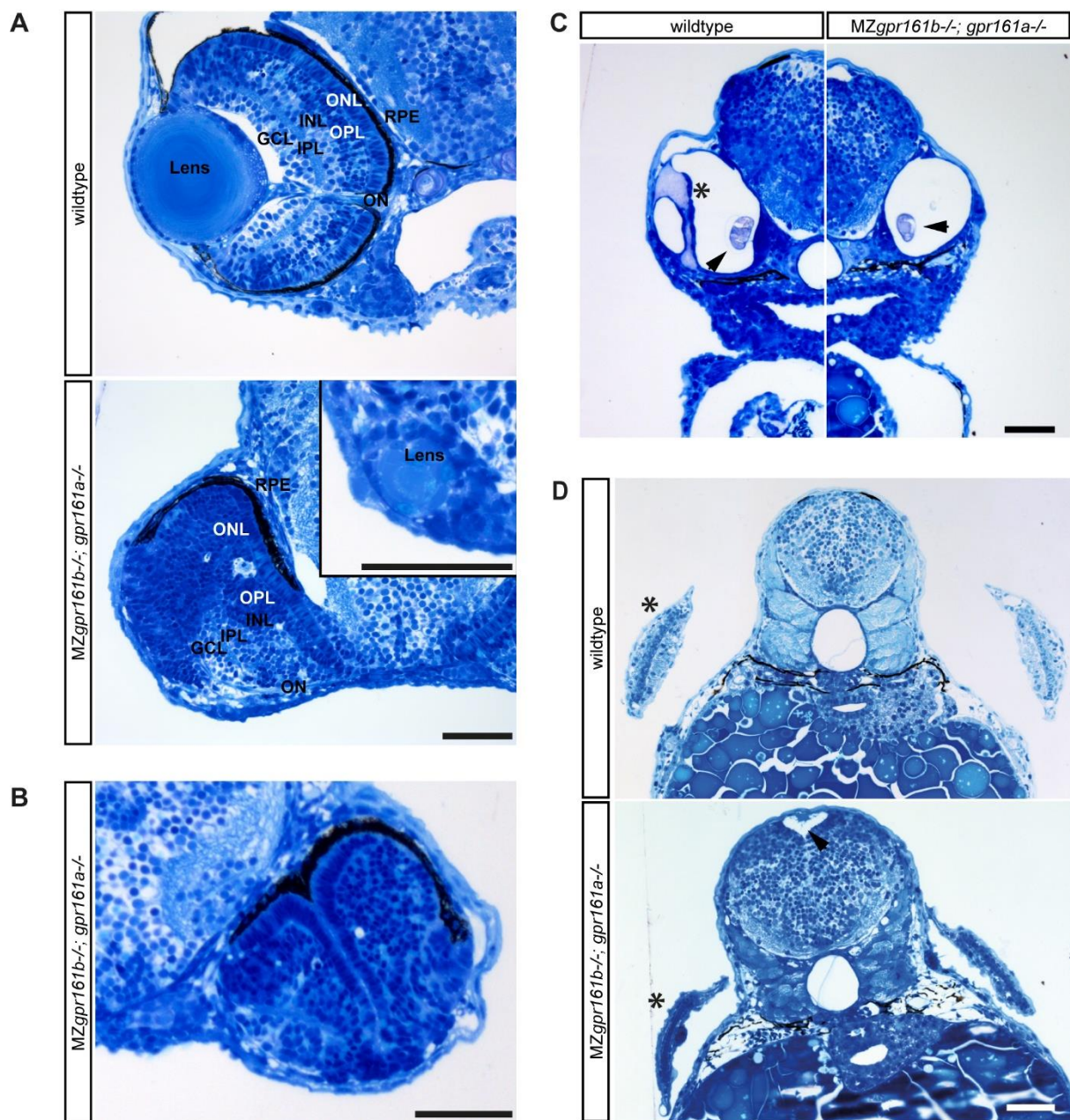
**Figure S2. CRISPR knock out strategy.**

Schematic representation of the gene structure of *gpr161a* (A) and *gpr161b* (B) indicating the position of CRISPR sgRNA recognition site and a sequence alignment of the obtained mutant alleles.



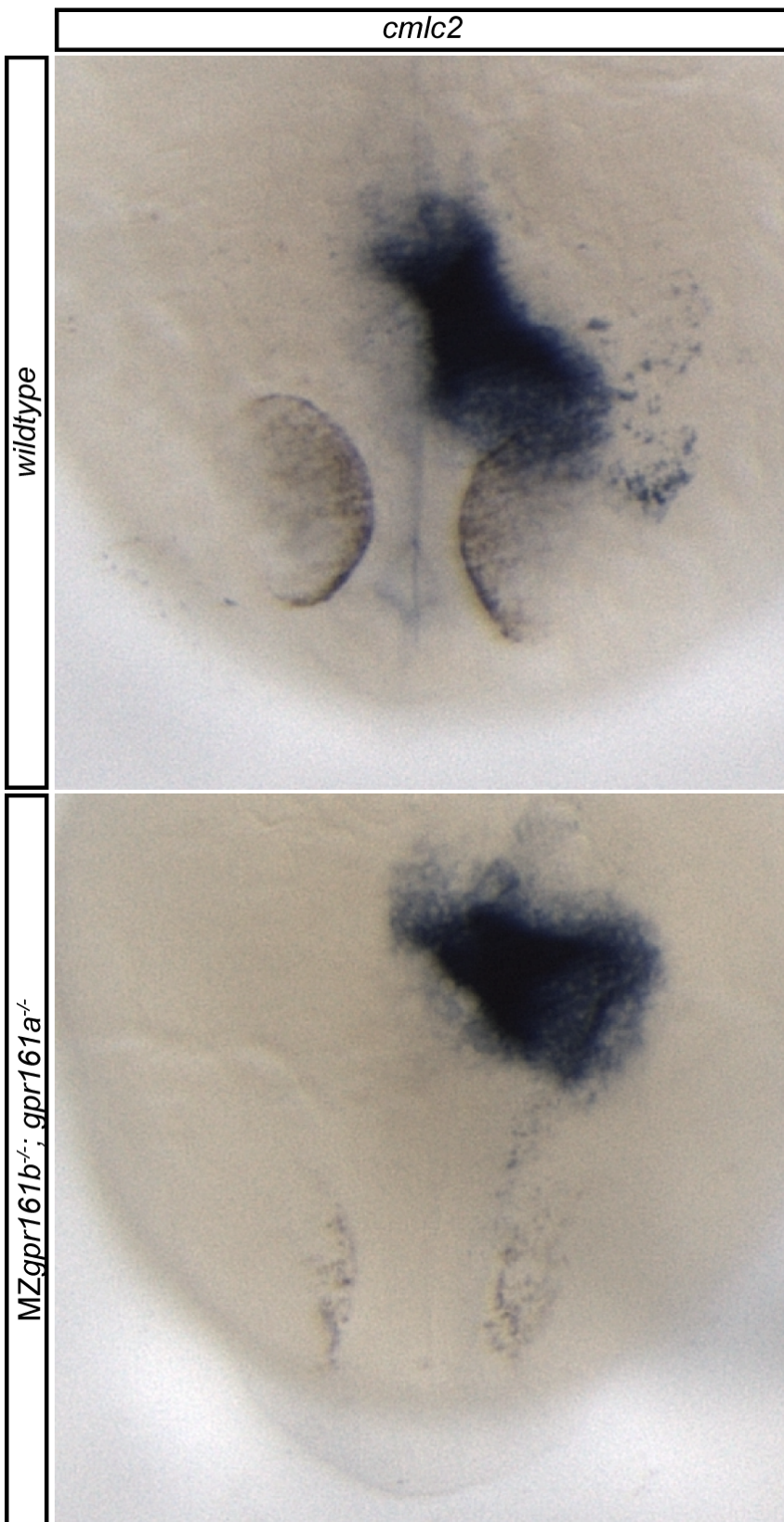
**Figure S3. Maternal loss of *gpr161b* does not lead to genetic compensation by *gpr161a*.**

Transcript levels of *gpr161a* and *gpr161b* in single embryos at 2-cell stage as determined by qRT-PCR (n=6 embryos for each experiment; \*\* P<0.01, ns not significant, Kruskal-Wallis rank sum test, Dunn's post hoc test for multiple comparisons). *gpr161a*<sup>??</sup> indicates that the embryos used were not genotyped for *gpr161a*.



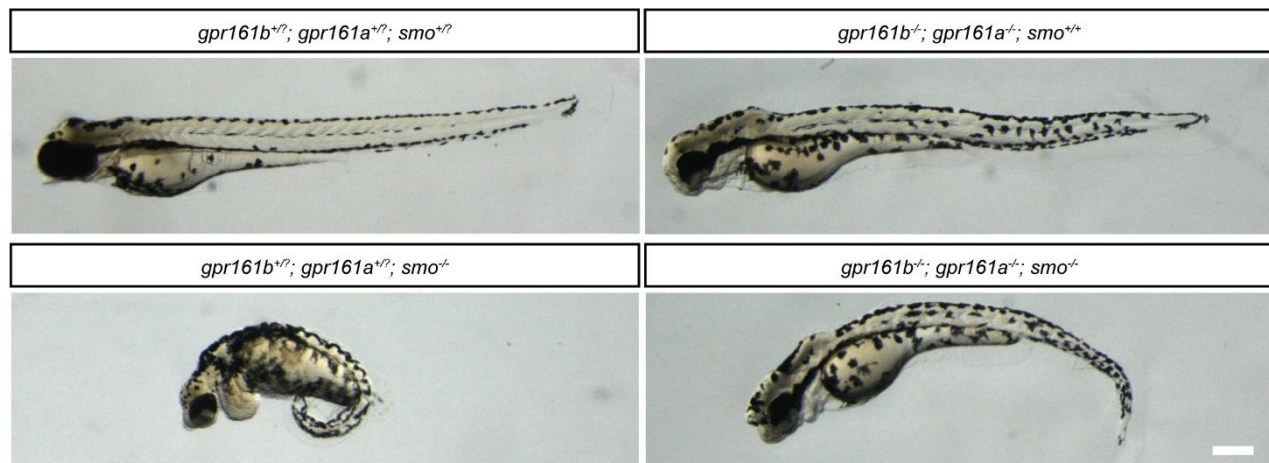
**Figure S4. Severe morphological defects in *gpr161* mutant embryos at 72 hpf.**

(A) Transverse section through the embryonic eye at 72 hpf. Retinal layers are indicated as follows: RPE – retinal pigment epithelium, ONL – outer nuclear layer, OPL - outer plexiform layer, INL – inner nuclear layer, IPL inner plexiform layer, GCL ganglion cell layer. Inset shows remnant of a forming lens from a different section of the same *gpr161* mutant embryo. (B) Transverse section through the embryonic eye of a 72 hpf *gpr161* mutant embryo shows a conspicuous invagination of the outer retinal layers. (C) Transverse section through the otic capsule of wildtype and *gpr161* mutant embryos at 72 hpf. Asterisk highlights central canal and dorsolateral septum which are missing in *gpr161* mutant embryos. Arrowhead shows otholiths. (D) Transverse section through the hindbrain region of wildtype and *gpr161* mutant embryos at 72 hpf. Asterisks highlight presence of pectoral fins. Arrowhead shows enlarged brain ventricle. An increase in hindbrain diameter can be noted. (all scale bars: 50μm)



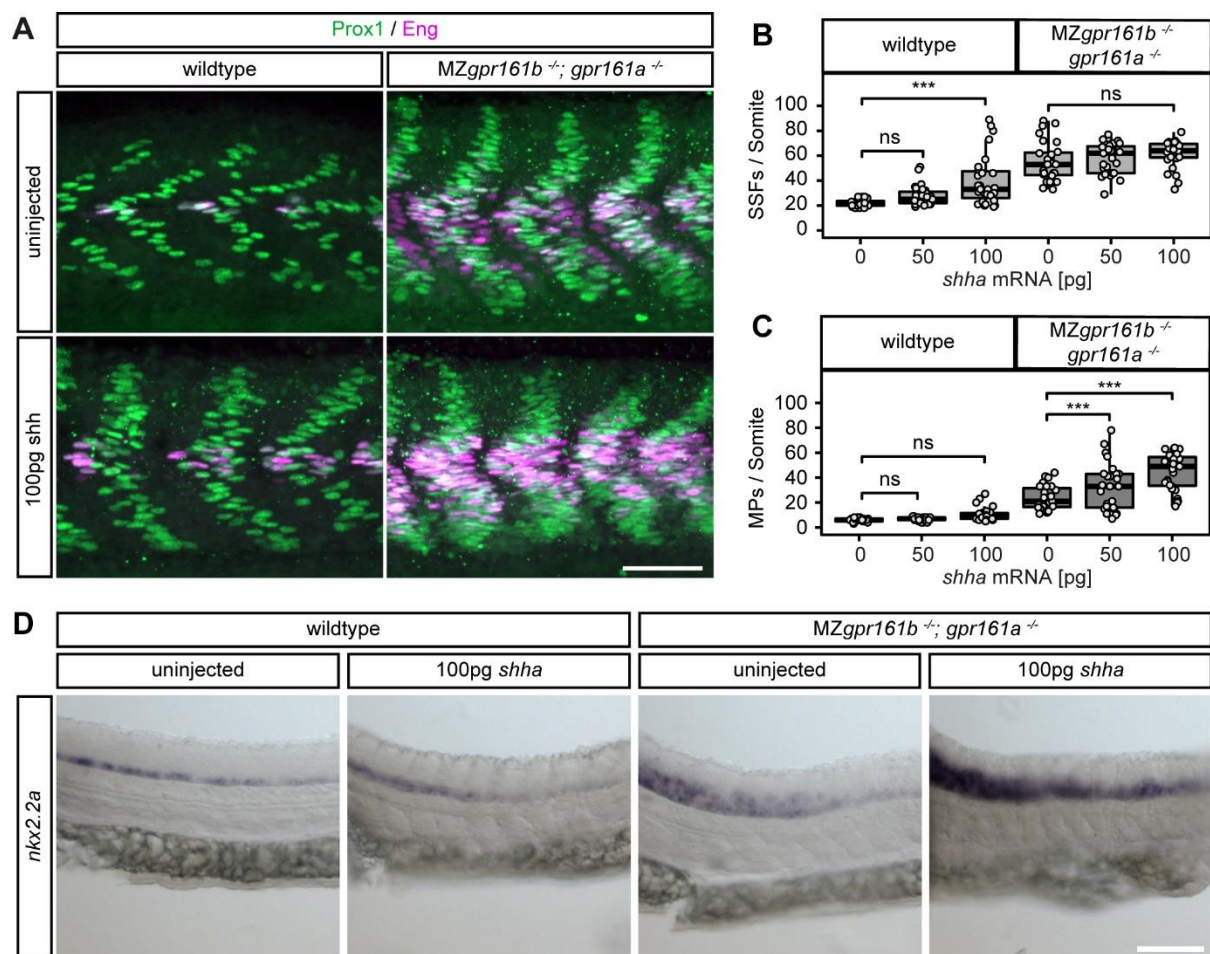
**Figure S5. Laterality is not affected in *gpr161* mutants.**

In-situ hybridization of *cmlc2* transcripts at 24hpf in wildtype and *gpr161b<sup>-/-</sup>; gpr161a<sup>-/-</sup>* mutant embryos.



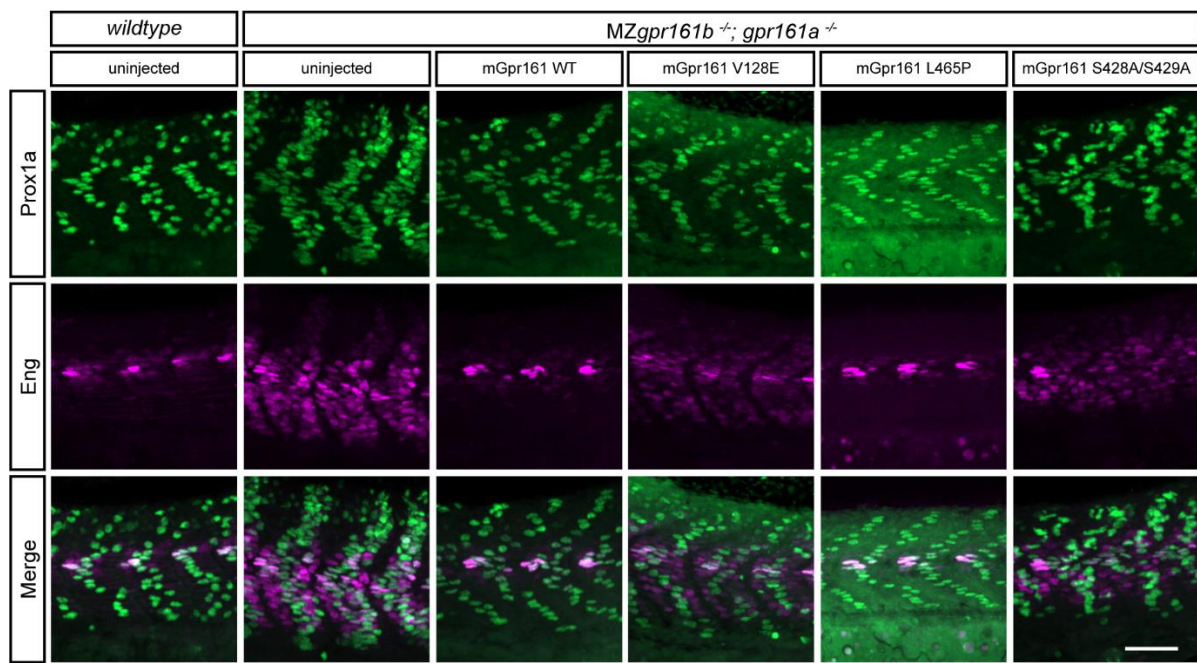
**Figure S6. Morphological phenotypes of *gpr161b*<sup>-/-</sup>; *gpr161a*<sup>-/-</sup> mutants are independent of Smo.**

Lateral view of embryos from a *gpr161b*<sup>+/-</sup>; *gpr161a*<sup>+/-</sup>; *smo*<sup>+/+</sup> incross at 72hpf (scale bar: 100μm).



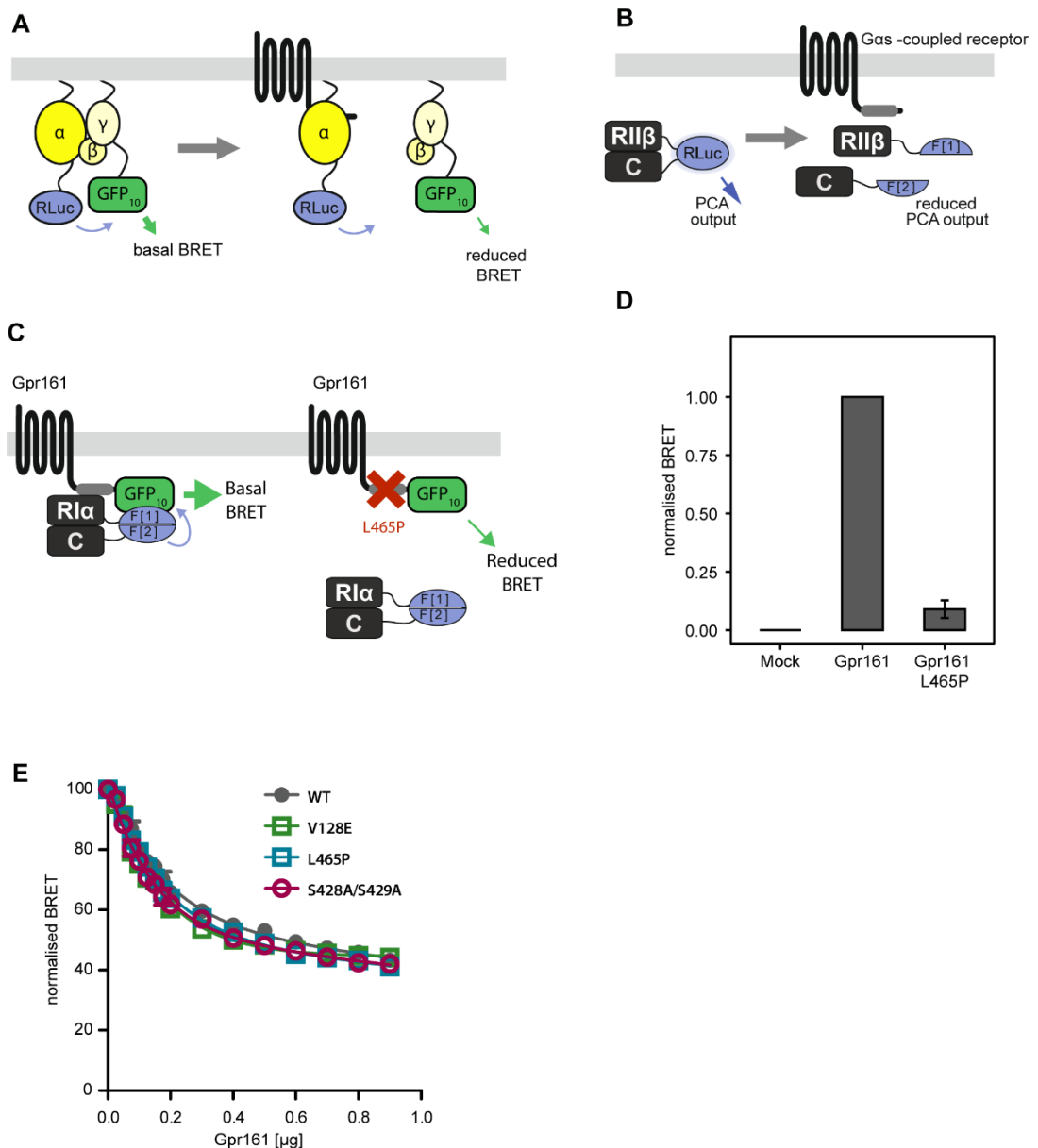
**Figure S7. Injection of *shh* mRNA can elevate hh signalling outcomes in *gpr161* mutants.**

(A) Prox1 (green)/ Eng (purple) immunostainings of wild-type and MZgpr161b<sup>-/-</sup>; gpr161a<sup>-/-</sup> embryos injected with 100 pg of *shha* mRNA (scale bar: 50μm). (B-C) Quantification of SSFs and MPs in wild-type and MZgpr161b<sup>-/-</sup>; gpr161a<sup>-/-</sup> embryos injected with increasing amounts of *shh* mRNA (n=27 somites in 9 embryos; \*\*\* P<0.001, ns not significant, two-way ANOVA, Tukey's post-hoc test for pairwise comparisons). (D) RNA in situ hybridization of *nkx2.2a* transcripts in wildtype and MZgpr161<sup>-/-</sup>; gpr161<sup>-/-</sup> embryos at 24 hpf upon injection of 100pg *shha* mRNA (lateral view, scale bar: 100μm).



**Figure S8. Injection of mGpr161-mCherry rescues the somite phenotype of gpr161 mutants.**

Prox1 (green)/ Eng (purple) immunostainings of wild-type and MZgpr161b<sup>-/-</sup>; gpr161a<sup>-/-</sup> embryos injected with 100 pg of mGpr161-mCherry mRNA as indicated (scale bar: 50μm)

**Figure S9. BRET and PCA biosensors**

**(A)** Schematic of the three-component BRET biosensor (Galés et al., 2005; Thomsen et al., 2016): Gα fused to an RLuc protein serves as a photon donor, while GFP10 Gy acts as a photon acceptor, resulting in a measurable BRET signal when the trimeric G-protein complex Gαβγ is formed. Activation via GPCRs leads to the separation of Gα and Gβγ, reducing the BRET signal. **(B)** Schematic depiction of the PKA PCA assay, two fragments (F[1] and F[2]) of a split Renilla Luciferase (RLuc) are fused to the catalytic (C) and regulatory (RIIβ) subunits of PKA. When the holoenzyme is formed a functional RLuc is reconstituted resulting in high luciferase signals upon addition of a substrate. When PKA is activated the C subunit leaves the complex resulting in lower luciferase signals since protein complementation of F[1] and F[2] is abrogated **(C)** Schematic depiction of the PCA-BRET combination. PKA holoenzyme formation allows luciferase complementation and reconstitution generating a functional photon donor for GFP10 tagged Gpr161 which results in a BRET signal upon close contact. Two conditions are shown, either in the presence of Gpr161 wildtype or in the presence of Gpr161<sup>L465P</sup> which cannot bind RI. **(D)** HEK293 cells expressing PKA-RIα[F1] and PKA-C[F2] as well as GFP10-tagged Gpr161 variants were used for plate reader analyses ( $\pm$ SD of one representative experiment carried out in multiples). **(E)** Normalised BRET signal upon co-expression of the Gαβγ-BRET sensor and increasing concentrations of Gpr161 variants in HEK293 cells. Signal has been normalised to wildtype Gpr161, mock transfection signals were used for background subtraction (SD of n=5 independent experiments).

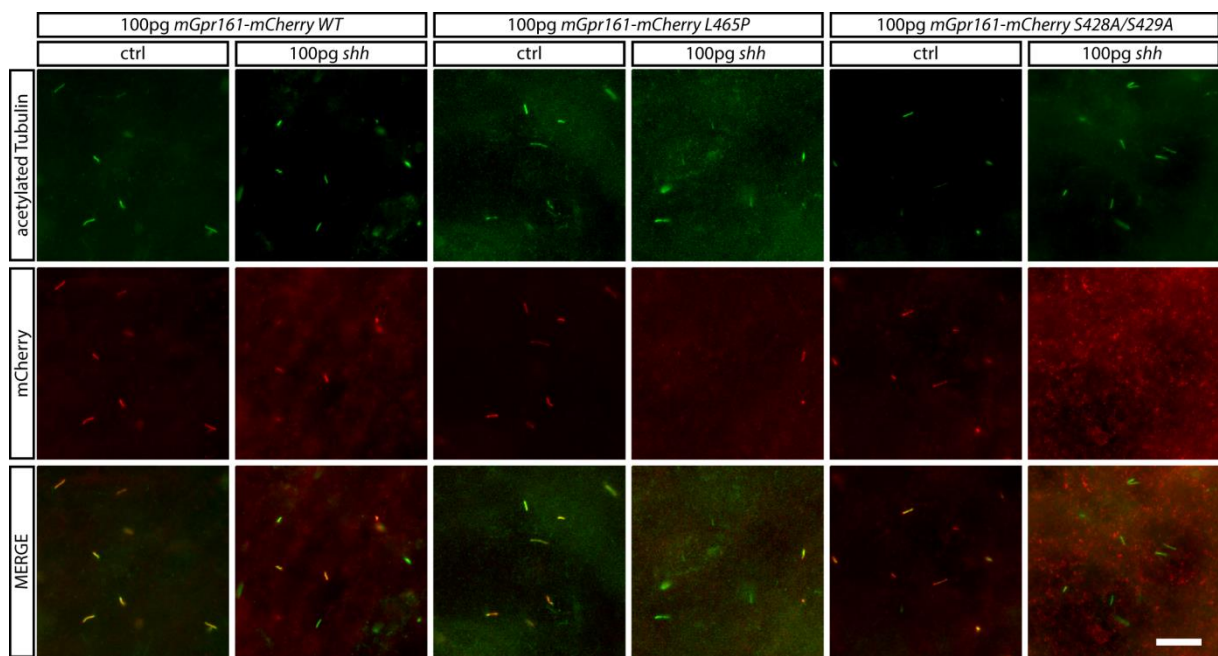


**Figure S10. PKA-phosphorylation mutants of mGpr161-mCherry show altered ciliary localisation upon co-injection of *shha* mRNA.**

Immunostainings of mCherry (red) and acetylated tubulin (AcTub, green) at 9hpf (scale bar: 10μm).

## Supplementary Tables

**Table S1.** List of Antibodies

Antibody	Source	Dilution	Identifier
Prox1	abcam	1:500	ab209849
Engr	DSHB	1:20	4D9
Myc	abcam	1:500	ab9106
acTub	Sigma	1:500	T7451
mCherry	S.Geley	1:500	
Alexa Fluor 647 anti mouse	ThermoFisher	1:500	A-21235
Alexa Fluor 488 anti rabbit	ThermoFisher	1:500	A-11008

**Table S2.** List of Primers

Name	Used for	Sequence
Gpr161a_SSPL_F	Genotyping	TGATCTGACTGAGGCCTTATGGG
Gpr161a_SSPL_R	Genotyping	AAGAGGATGACAAGCCGCACTG
gpr161b_SSPL_F	Genotyping	CACAAGGGATTGATTGAAATG
gpr161b_SSPL_R	Genotyping	ATTGCAAGCACAGCTCGATT
gpr161a-IVA-F	Cloning	AATTCAAGGGCAAACATGAACACCAGCAGCAATGA
gpr161a-IVA-R	Cloning	CACGGAGGCCACCTCCTGCGCATATTCCTCGATAT
gpr161b-IVA-F	Cloning	AATTCAAGGGCAAACATGAACGGCTCTAAGAATGG
gpr161b-IVA-R	Cloning	CACGGAGGCCACCTCCCATTTCCTCGCGCTCCA
mGpr161-V128E-F	Site-directed mutagenesis	GAGCTCTATCCAATGGTGTACCCC
mGpr161-V128E-R	Site-directed mutagenesis	GGCGTAGTAGCGATCGATGGC
gli1_qpcr_f	qPCR	GTAAGGCCACACACACACTGATG
gli1_qpcr_r	qPCR	GCTACACCCACAGTCCTTTG
nkx2.2b_qpcr_f	qPCR	GTGCGGACACAAATATCCAGTGC
nkx2.2b_qpcr_r	qPCR	ATCCGCGGACAGTTCTGGATTC
nkx6.1_qpcr_f	qPCR	GACAGAGAGTCAAGTCAAGGTGTG
nkx6.1_qpcr_r	qPCR	TCCTTCAGCCTCTCGGTTCTG
olig2_qpcr_f	qPCR	TGCACCTGCTACGGGAATATC
olig2_qpcr_r	qPCR	TGTCAGAGTCCATGGCGTTCA
pax7a_qpcr_f	qPCR	ACGGCATTCTGGGAGACAAAGGTC
pax7a_qpcr_r	qPCR	TGCGTCTCTGCTTCTTGAGC
eef1a1l1_qpcr_f	qPCR	TCTCTACCTACCCCTCTTGGTC
eef1a1l1_qpcr_r	qPCR	TTGGTCTTGGCAGCCTCTGTG
rpl13a_qpcr_f	qPCR	ACAGGCTGAAGGTGTTGATGGC
rpl13a_qpcr_r	qPCR	GGACAACCATGCGCTTCTTG
gpr161b_qpcr_F	qPCR	ATAAGAGGAGGAGCTCGGTAC
gpr161b_qpcr_R	qPCR	TGGACTACTGAAGGGTCACCTG
gpr161a_qpcr_F	qPCR	AGCATCTCCAACCGAATCACAG
gpr161a_qpcr_R	qPCR	CAACATGGTGTCTGTCCCTGAG